Int. J. Electrochem. Sci., 6 **(2011)** 3224 - 3237

International Journal of
ELECTROCHEMICAL
SCIENCE
www.electrochemsci.org

Amperometric Determination of Folic Acid at Multi-Walled Carbon Nanotube-Polyvinyl Sulfonic Acid Composite Film Modified Glassy Carbon Electrode

Binesh Unnikrishnan, Yan-Ling Yang, Shen-Ming Chen[*]

Electroanalysis and Bioelectrochemistry Lab, Department of Chemical Engineering and Biotechnology, National Taipei University of Technology, No. 1, Section 3, Chung-Hsiao East Road, Taipei 106, Taiwan, ROC
[*]E-mail: smchen78@ms15.hinet.net

Received: 15 June 2011 / *Accepted:* 6 July 2011 / *Published:* 1 August 2011

We investigated the electrochemical reduction behavior of folic acid (FA) at multi-walled carbon nanotube-polyvinylsulfonate (MWCNT-PVS) composite film modified glassy carbon electrode (GCE) using cyclic voltammetry (CV). FA undergoes a $2e^-/2H^+$ transfer electrochemical reduction process at –0.7 V with respect to Ag/AgCl reference electrode in pH 7. The reduction peak current increased linearly with the increase in concentration of FA. So far no reports are available for the amperometric determination of FA utilizing the reduction process occurring at negative over potential (– 0.7 V). We attempted the amperometric studies making use of this reduction process at –0.7 V. MWCNT-PVS modified electrode showed good amperometric response in the wide linear range from 5.3×10^{-5} M to 1.7×10^{-3} M with a sensitivity of 0.1737 μA $\mu mol^{-1} cm^{-2}$. The surface morphology of MWCNT-PVS film was done by scanning electron microscopy (SEM) and the interfacial electron transfer phenomenon at the modified electrode surface was studied using electrochemical impedance spectroscopy (EIS). The studies showed that MWCNT is well dispersed in PVS and the composite film possesses less electron transfer resistance making it a promising material for electrocatalytic and biosensing applications.

Keywords: Folic acid, electrochemical reduction, multi-walled carbon nanotubes, cyclic voltammetry, amperometry

1. INTRODUCTION

Folic acid (FA) is a B-group vitamin which has a major role in biological functions of cell metabolism like DNA replication, repair and methylation, synthesis of nucleotides, vitamins, amino acids etc. An inadequate intake of folates in human beings is associated with an increased risk of colorectal cancer [1] and a risk factor for neural tube defects [2]. FA deficiency can also affect the

stability of DNA by altering the DNA methylation process, a situation called hypomethylation [3] and it potentially induces proto-oncogene expression leading to cancer [4]. DNA can also be seriously damaged by free radical attacks. So, an adequate antioxidant level is essential for cell health. Folates possess antioxidant properties that protect the genome by inhibiting free radical attack of DNA in addition to their role in DNA repair and replication mechanisms [5]. Therefore, intake of folates through tablets and fortified foods is essential for the population suffering from folate deficiency. The most stable folate form is FA. It is cheap to synthesize and is thus frequently used for food fortification and in supplements. Hence, FA determination is important and essential in food & pharmaceutical industries and also in clinical laboratories. Chemically, folic acid is {N-[4-(2-amino-l,4-dihydro-4-oxo-6-pteridinyl)methyl)amino) benzoyl] –L glutamic acid}. The chemical structure of FA is given in scheme 1. For our convenience of writing the equation of reaction and further discussions one part of FA structure is labeled as pteridine ring and the remaining side chain as R.

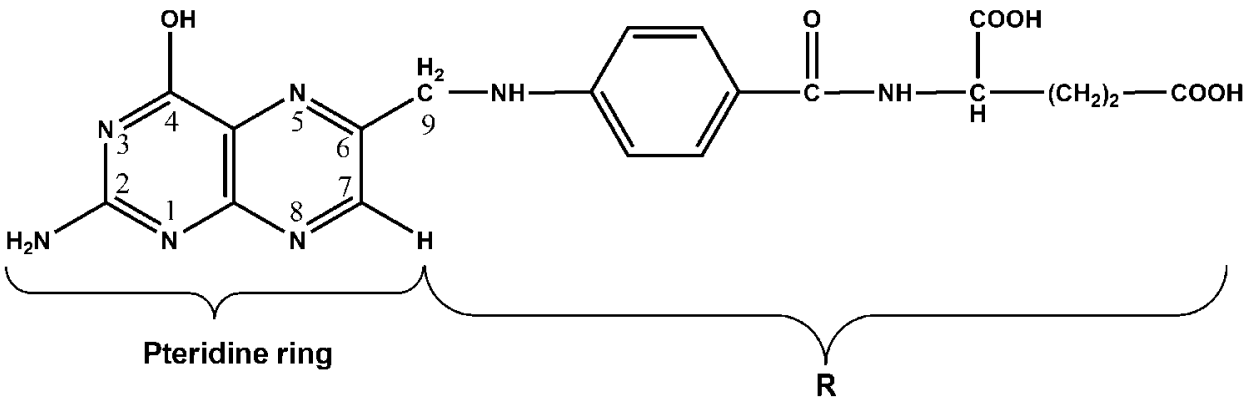

Scheme 1. Chemical structure of FA

Various electrochemical methods have been employed for the study of direct electrochemistry of FA and its determination [6-8]. Cakir et *al*. [9] studied the simultaneous determination of FA and riboflavin in pharmaceutical samples by square wave voltammetry (SWV). Kalimuthu et *al*. [10] used ultrathin electropolymerized film of 5-amino-2-mercapto-1,3,4-thiadiazole modified glassy carbon electrode for the selective determination of FA in common physiological interferents by differential pulse voltammetry (DPV) and amperometry. Methods like SWV, DPV [11, 12] chronoamperometry [13, 14] and differential pulse cathodic stripping voltammetry [15] were used for the FA determination studies. FA has been simultaneously determined along with norepinerphrine [16], uric acid [17] and ascorbic acid [18] by DPV at modified carbon nanotube paste electodes. However, very few reports of amperometric i-t curve studies are available for FA.

Carbon nanotubes (CNT) have been extensively used in electrode modification for electrochemical studies, due to their high specific surface area, excellent structural, electronic and mechanical properties. However, producing homogeneous dispersion of CNT in polar solvents is difficult due to its hydrophobic nature. Therefore, in many cases CNT is used after pretreatment or functionalization. Previous reports show that electrodes modified with pretreated CNT exhibit very

good catalytic activity towards the electrochemical oxidation of substances like phenolic compounds [19-21], alkaloids [22] etc. CNT modified electrodes also provide a faster electron transfer rate and catalytic activity towards many important biomolecules [23-25]. Surfactants are often used to prepare homogeneous CNT dispersion. The use of surfactants is also very common in the fabrication of biosensors. In some cases surfactant film also acts as a membrane protecting the electroactive species. The electrochemistry of electroactive molecules embedded in surfactant film has been studied extensively [26-30]. The surfactant film facilitates the electron transfer from the reactants or the electroactive species to the electrode. It also blocks some interferants and thus helps to improve the selectivity of the modified electrode. Cheng et *al*. studied the direct electrochemistry of hemoglobin at Poly (styrene sulfonic acid) (PSS) and single-walled carbon nanotube (SWCNT) modified Au electrode and observed that both SWCNT and PSS could accelerate the electron transfer between Hb and the electrode [31]. Similarly, PSS/MWCNT modified GCE shows good selective electrocatalytic activity towards dopamine in presence of ascorbic acid [32].

To date, reports are available for determination of FA at MWCNT modified electrodes by CV, Chronoamperometric and Chronocoulometric methods [33]. Amperometric determination of FA at thiadiazole modified GCE at positive potential 0.9 Vis also reported [10]. However, to our knowledge, little reports are available for the amperometric i-t curve studies of FA at MWCNT modified GCE. So, in this study we attempted to develop an amperometric sensor for FA determination using MWCNT and poly (vinylsulfonate) (PVS) composite. We prepared a homogeneous and stable dispersion of MWCNT using PVS as the dispersing medium. The MWCNT-PVS composite modified GCE exhibits excellent amperometric response to FA at negative over potential with good sensitivity and linear range.

2. MATERIALS AND METHODS

2.1. Apparatus

The cyclic voltammetric experiments were carried out using a CHI 611A electrochemical workstation. A conventional three electrode system with MWCNT, PVS and MWCNT-PVS modified GCE as working electrodes, a thin Pt wire as counter electrode and Ag/AgCl (sat. KCl) as reference electrode was used. Electrochemical impedance spectroscopy (EIS) measurements were done using IM6ex ZAHNER (Kroanch, Germany). Scanning electron microscopy (SEM) was performed using a Hitachi S-3000 H Scanning Electron Microscope. A CHI 750 potentiostat with analytical rotator AFMSRX (PINE Instruments, USA) was used for amperometric experiments.

2.2. Reagents and materials

MWCNT with O.D. 10 – 15 nm, I.D. 2–6 nm and length 0.1–10 μm was obtained from Sigma–Aldrich. Folic acid dehydrate (97%) and poly(vinylsulfonic acid, sodium salt) 25% solution in water were obtained from Aldrich, USA. 0.1 M phosphate buffer solution (PBS) was prepared from 0.1 M

Na_2PO_4 and NaH_2PO_4 in doubly distilled deionized water to get a pH of 7. Inert atmosphere was set by passing N_2 over the solution during experiment. All the experiments were conducted at ambient temperature (25ºC ± 2ºC).

2.3. Preparation of MWCN-PVS composite modified electrode

Dispersing MWCNT in aqueous solution is difficult. However, pretreated MWCNT forms stable and homogeneous MWCNT dispersion in polar solvents. MWCNT was pretreated adapting the procedures reported elsewhere [34, 35]. In a typical process, 150 mg of MWCNT was heated at 350ºC for 2 h and allowed to cool down to room temperature. Then it was ultrasonicated for 4 h in concentrated HCl to remove impurities like amorphous carbon and metal catalysts. It was filtered and washed thoroughly with deionized water until the pH of the washing was 7. The filtered MWCNT was dried at 100ºC for 1 h. The purified MWCNT was treated by ultrasonication in a mixture of sulfuric acid and nitric acid in 3:1 ratio for 6 h. It was then washed several times with deionized water, until the washing was neutral and dried. 1 mg of the pretreated MWCNT was dispersed into 1 mL of 1% PVS solution by ultrasonication for 30 min. A well dispersed homogeneous solution of 1 mg mL^{-1} MWCNT in PVS was obtained. To fabricate the MWCNT-PVS modified electrodes, the GCE was polished using 0.05 μm alumina slurry and Buehler polishing cloth. The GCE was washed and then ultrasonicated in deionized water and ethanol for 5 min each to remove any adsorbed alumina particles on the electrode surface. 3 μL of MWCNT-PVS dispersion was drop casted onto the well polished GCE surface and dried at 50ºC. Same conditions were used to fabricate MWCNT/GCE and PVS/GCE for comparison.

3. RESULTS AND DISCUSSIONS

3.1. Electrochemical behavior of FA at various electrodes

Fig. 1 shows the cyclic voltammetric behavior of FA at various electrodes in 0.1 M PBS (pH 7). Cyclic voltammograms were recorded in the potential range of –0.2 to –1.25 V vs. Ag/AgCl reference electrode at a scan rate of 0.1 Vs^{-1}. In prior to each experiment, purified N_2 was purged into PBS containing 100 μM FA for 10 min. FA shows a well-defined cathodic peak at MWCNT-PVS/GCE (d) at –0.70 V. Wang, et *al*. [36] reported two couples of redox peaks and an irreversible reduction peak between 0.4 and -1.4 V for FA at SWCNT modified electrode in pH 5.5. Jiang et *al.* [7] observed a pair of oxidation and reduction peaks at MWCNT modified GCE with ΔE_p 0.061 V and with a peak current ratio of 1:1, in the potential range of -0.6 to -0.2 V in pH 6.4 PBS. Cakir et *al*. reported three cathodic peaks for FA at –0.4, –0.87 and –1.2 V in pH 5.89 at a static mercury drop electrode using SWV. Their results also suggest that the peaks at –0.4 and –1.2 V are not good enough for analytical purpose but the peak at –0.87 V is well developed and provide the basis for quantitative determination of FA [9]. However, we observed a single reduction peak at –0.70 V at MWCNT-PVS/GCE in the potential range of –0.2 to –1.2 V. This cathodic peak is attributed to the reduction of

FA by $2e^{-}/2H^{+}$ reduction process in which FA is converted to 5, 8-dihydro FA [37, 38]. The reduction of FA at – 0.7 V takes place as per the equation given in scheme 2.

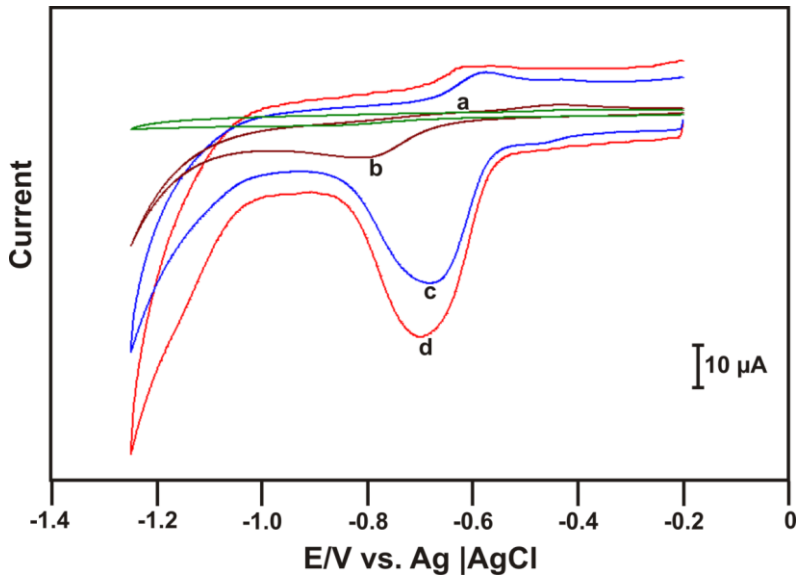

Figure 1. Cyclic voltammograms of FA (100 µM) at a) bare GCE, b) PVS/GCE, c) MWCNT/GCE and MWCNT-PVS/GCE in N_2 saturated 0.1 M PBS (pH 7). Scan rate: $0.1Vs^{-1}$.

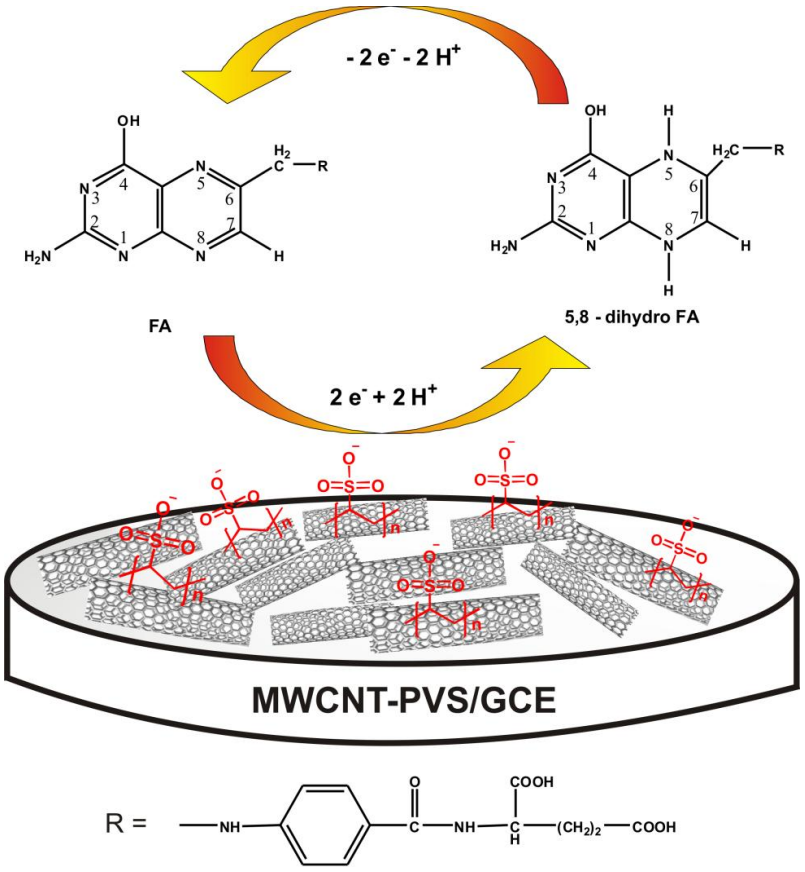

Scheme 2. Electrocatalytic reduction of FA to 5, 8-dihydro FA at MWCNT-PVS/GCE in pH 7 PBS.

From fig.1 (c) and (d) it is clear that MWCNT-PVS/GCE shows an enhanced cathodic peak than MWCNT/GCE at –0.7 V. This could be due to PVS facilitating the electron transfer process. In contrast, PVS/GCE (b) exhibits the cathodic peak at –0.815 V with much lesser current. Bare GCE (a) too shows a very less prominent reduction peak for FA at –0.883V. On comparison with the bare GCE, a183 mV shift in peak potential and the increase in peak current demonstrates the efficient electrocatalytic behavior of MWCNT-PVS composite film towards the reduction of FA with good background current stability. Hence, the cathodic peak at – 0.7 V is well developed and could be used for the quantitative and qualitative determination of FA.

3.2. Electrocatalytic reduction of FA at MWCNT-PVS/GCE

Fig.2 shows the cyclic voltammograms obtained for various concentration of FA at MWCNT-PVS/GCE. The cathodic peak current, (I_{pc}) increases with the increase in concentration of FA from 2 to 521 µM. The linear dependence of I_{pc} to concentration of FA is given in inset of fig. 2.

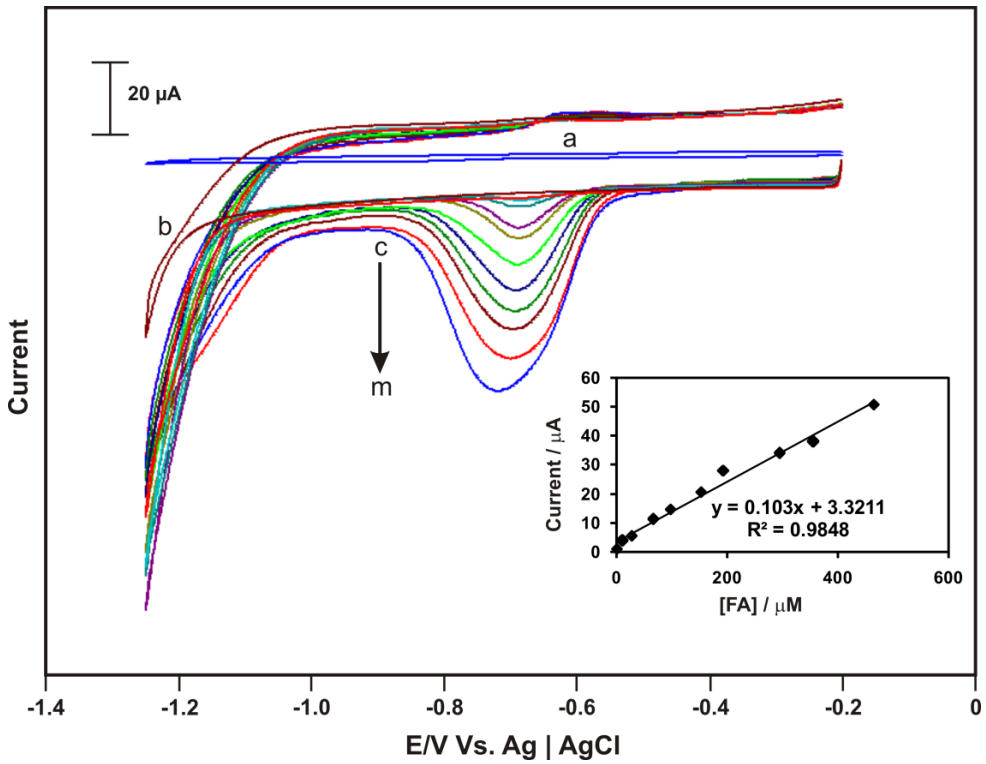

Figure 2. Cyclic voltammogram obtained at (a) bare GCE in the presence of 521 µM FA in N_2 saturated 0.1 M PBS (pH 7). Cyclic voltammogram obtained at MWCNT-PVS/GCE (b) 0, c) 2, d), 12, e) 29, f) 67, g) 99, h) 154, i) 193, j) 296, k) 355, l) 465, and m) 521 µM FA in same condition as (a). Inset shows the plot of I_{pc} vs. FA concentration. Scan rate: 0.1Vs^{-1}.

I_{pc} increases linearly with FA concentration with a slope of 0.103µA μM^{-1} and the linear regression coefficient, R^2 = 0.9848. The above result shows the stability of the film for electrocatalytic

applications in which the analyte is added continuously for many additions. Therefore we utilized this property of the film to conduct the amperometric i-t curve studies in section 3.7.

3.3. Influence of pH

Fig. 3 represents the cyclic voltammograms of 100 µM FA at MWCNT-PVS/GCE in the pH range from 1 to 13 at a scan rate of 0.1 Vs^{-1}. FA exhibits well defined cathodic peak in higher pH. Similar peak for FA at pH 7.4 was reported earlier by Cakir et *al*. [39]. E_{pc} of FA shifts to more negative potential with increase in pH. The inset of fig. 3 shows the linear dependence of pH on E_{pc}.

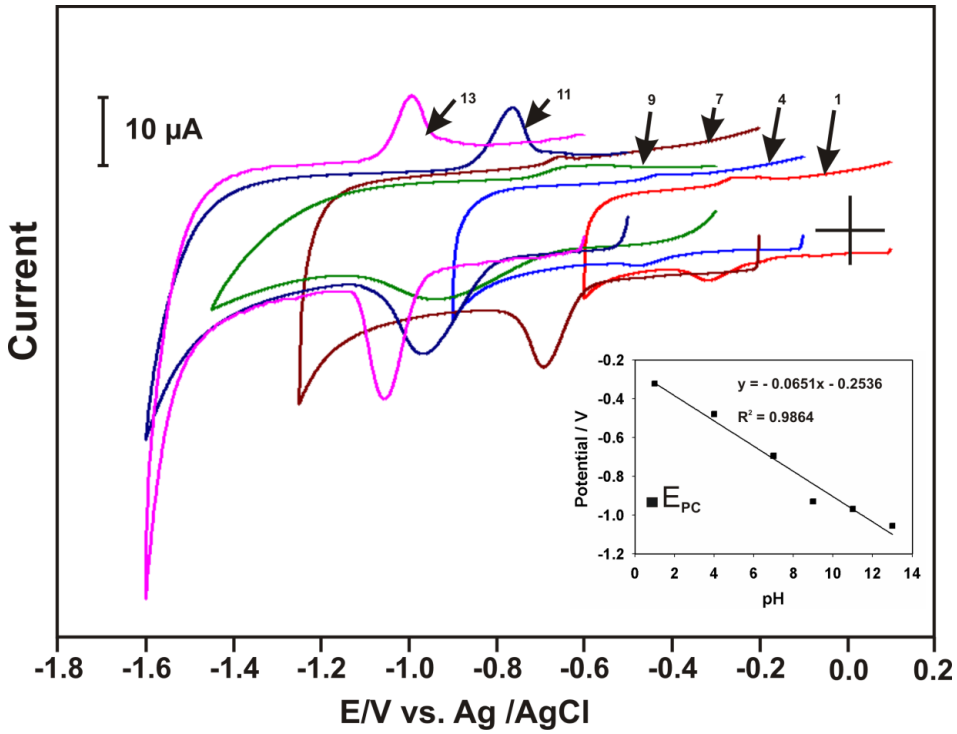

Figure 3. Cyclic voltammograms of MWCNT-PVS modified GCE in N_2 saturated various pH (1, 4, 7, 9, 11 and 13) solutions containing 100 µM FA at scan rate of 0.1 Vs^{-1}. Inset shows the influence of pH on E_{pc}.

It shows a slope value of 65 mV pH^{-1}, which is close to the theoretical value of equal number of electron and proton transfer process. This result confirms the $2e^{-}/2H^{+}$ reduction process. This reduction step of FA has been well explained by Gurira et *al*. [37] and Gall et *al*. [38].

3.4 Different scan rate studies for MWCNT-PVS/GCE

The different scan rate studies were conducted for MWCNT-PVS/GCE using CV in 0.1 M PBS (pH 7) containing 100 µM FA in the potential range of –0.2 to –1.25 V. Fig. 3 shows the cyclic voltammograms obtained for FA at different scan rates from 0.1 to 1.0 V. At lower scan rates the

anodic peak was not observed but it becomes more prominent at higher scan rates. As observed in section 3.3, at pH 11 and above the anodic peak observed even for lower scan rate 0.1 Vs^{-1}.

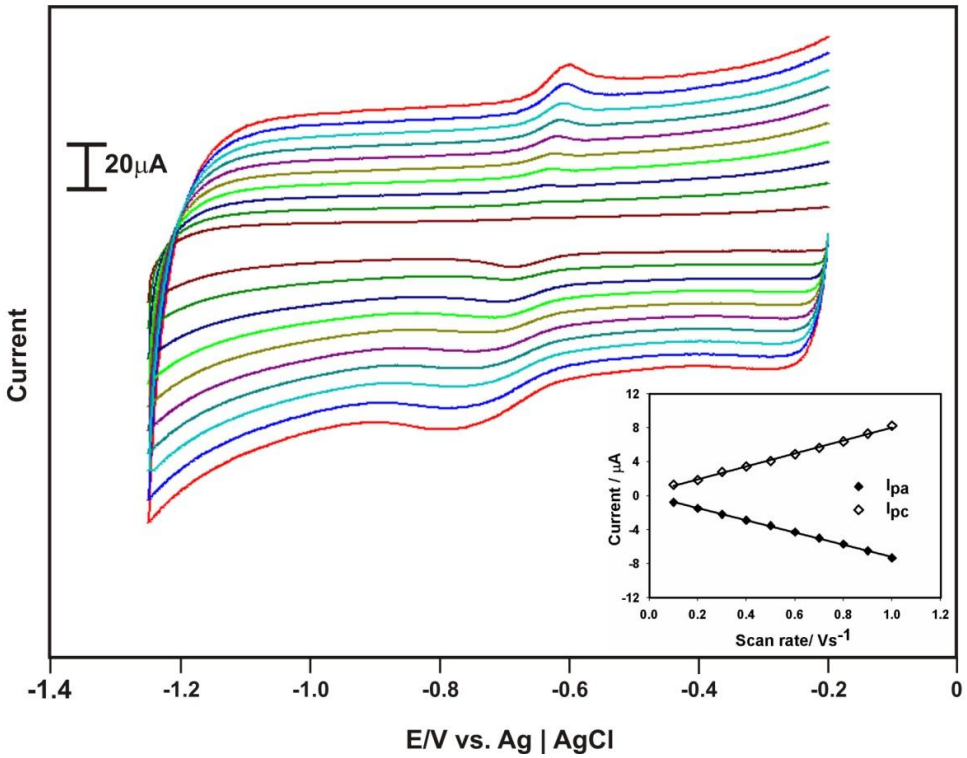

Figure 4. Cyclic voltammograms recorded at MWCNT- PVS/GCE in N_2 saturated 0.1 M PBS (pH 7) in presence of 100 μM FA at different scan rates. From inner to outer: 100, 200, 300, 400, 500, 600, 700, 800, 900 and 1000 mVs^{-1}. The inset shows the linear dependence of I_{pc} and I_{pa} on scan rates.

These results show an electrochemical reaction followed by a chemical reaction [37]. Both I_{pc} and I_{pa} increases linearly with the scan rate. The linear dependence of I_{pc} and I_{pa} with the scan rate is given in the inset. This result shows that the electrochemical process is surface confined. Since we are concerned on the reduction peak current only, we choose the scan rate 100 mVs^{-1} for all the CV experiments in this study.

3.5. EIS studies of different films

Conducting polymers, polyelectrolytes, nanomaterials or semiconducting materials coated on the electrode surface change the double layer capacitance and interfacial electron transfer resistance of the corresponding electrode. Impedance spectroscopy can reveal the interfacial changes due to the surface modification of electrodes [40]. The electrochemical impedance properties of the bare GCE, MWCNT, PVS, MWCNT-PVS modified GCE are recorded in 5mM $Fe(CN)_6^{3-}$/$FE(CN)_6^{4-}$ in PBS and are represented as Nyquist plot (Z_{im} vs. Z_{re}) in fig. 5. The inset of fig. 5 shows the Randles equivalence

circuit model used to fit the experimental data. Where R_s is the electrolyte resistance, R_{et} is charge transfer resistance, C_{dl} double layer capacitance and Z_w is Warburg impedance. The semicircle appeared in the Nyquist plot indicates the parallel combination of R_{et} and C_{dl} resulting from electrode impedance [41]. The semicircles obtained at lower frequency represent a diffusion limited electron transfer process and those at higher frequency represent a charge transfer limited process. From fig. 5, it is evident that bare GCE and PVS/GCE exhibit a semicircle at lower frequency region showing significant resistance towards the electron transfer process at the electrode surface. Whereas, MWCNT and MWCNT-PVS modified GCE exhibit a very small semicircle region indicating very low impedance of the films.

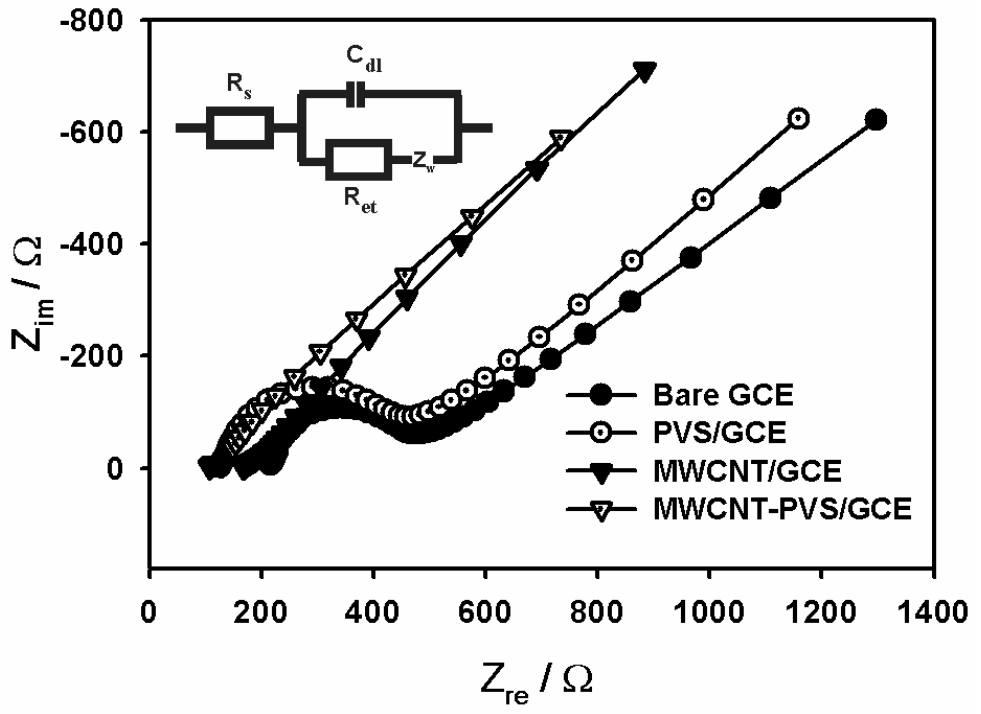

Figure 5. EIS of bare GCE, MWCNT, PVS and MWCNT-PVS modified GCE in 5mM $Fe(CN)_6^{3-}$ /$Fe(CN)_6^{4-}$ in 0.1 M PBS (pH 7). Applied AC voltage: 5mV, frequency: 0.1 Hz to 100 kHz.

This result is due to MWCNT providing a high rate of electron transfer. It also indicates that the PVS in the MWCNT-PVS composite film does not hinder the transfer of electrons and it maintains the conductivity of CNT.

3.6. Surface morphological characterization of various films using SEM

Dispersion of as purchased MWCNT in aqueous PVS solution was difficult due to its highly hydrophobic nature. The sonochemical treatment mentioned in section 2.3 generates oxygen containing functionalities such as quinones at the edge plain of the MWCNT [42]. These functional

groups give hydrophilic nature to the MWCNT and thus a homogeneous dispersion of MWCNT in PVS was obtained.

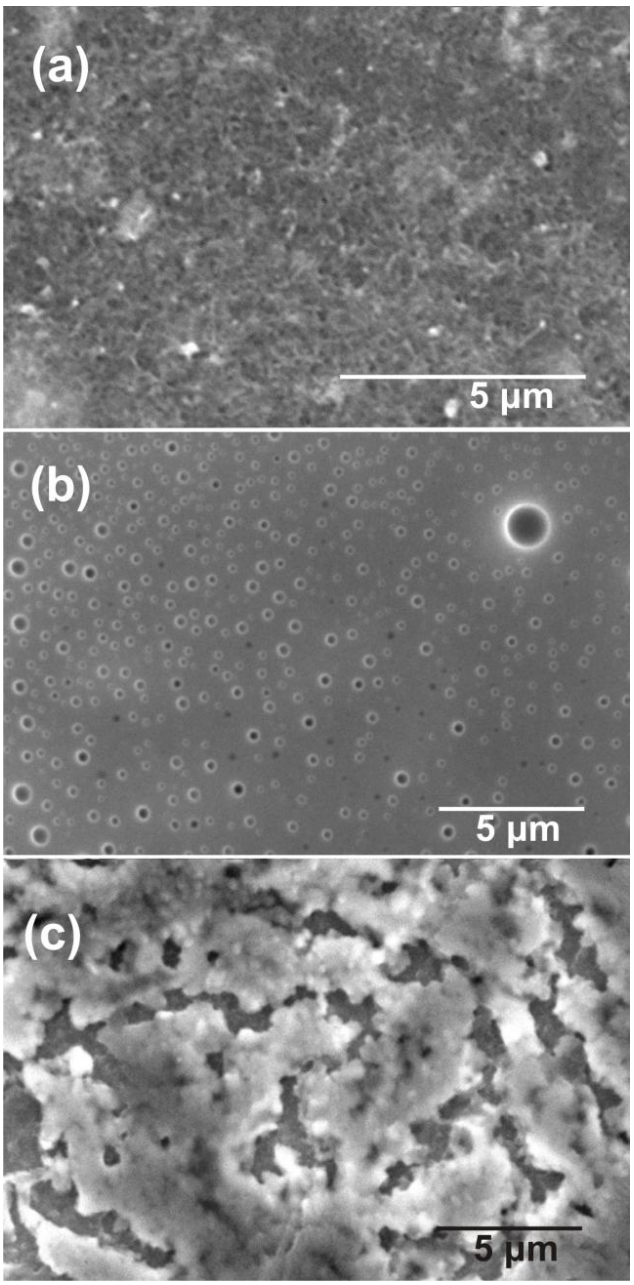

Figure 6. SEM images of a) MWCNT, b) PVS and c) MWCNT-PVS films

Fig. 6 shows the SEM images of MWCNT, PVS, and MWCNT-PVS films coated on indium tin oxide (ITO) electrode with identical conditions mentioned for the GCE modification. Comparison of the SEM images of the three films shows that there is morphological difference among them. Fig.6 (a) reveals the random distribution of MWCNT on ITO. The sonication process helps to unlock the MWCNT bundles into more simple strands of MWCNTs. Fig.6 (b) shows a very fine and thin distribution of porous PVS film over ITO. Fig.6 (c) shows a three dimensional MWCNT- PVS

structure. This indicates the formation of MWCNT-PVS composite. The three dimensional network allows good affinity for FA.

3.7 Amperometric detection of FA at MWCNT-PVS/GCE

Rotating disc electrode is a hydrodynamic electrochemical technique which involves the convective mass transport of reactants and products at the electrode surface, when the electrode is rotated at a specific speed [43]. Fig. 7 represents the amperometric response of FA at MWCNT-PVS modified RDE with surface area of 0.236 cm^2. The experiment was conducted in pH 7 (0.1M PBS) at an applied potential of –0.7 V with a rotation rate of 900 RPM. 1×10^{-2} M FA solution in pH 7 PBS was added at regular intervals of time. Electrocatalytic reduction of FA occurs at RDE in a totally mass transfer controlled condition. For every addition of FA, a quick response was observed and the reduction current increases linearly up to 3000 s which is equal to 1.7×10^{-3} M FA. An enlarged view of the amperometric response is shown in the inset (a) of fig.7. The amperometric response time is 5 s.

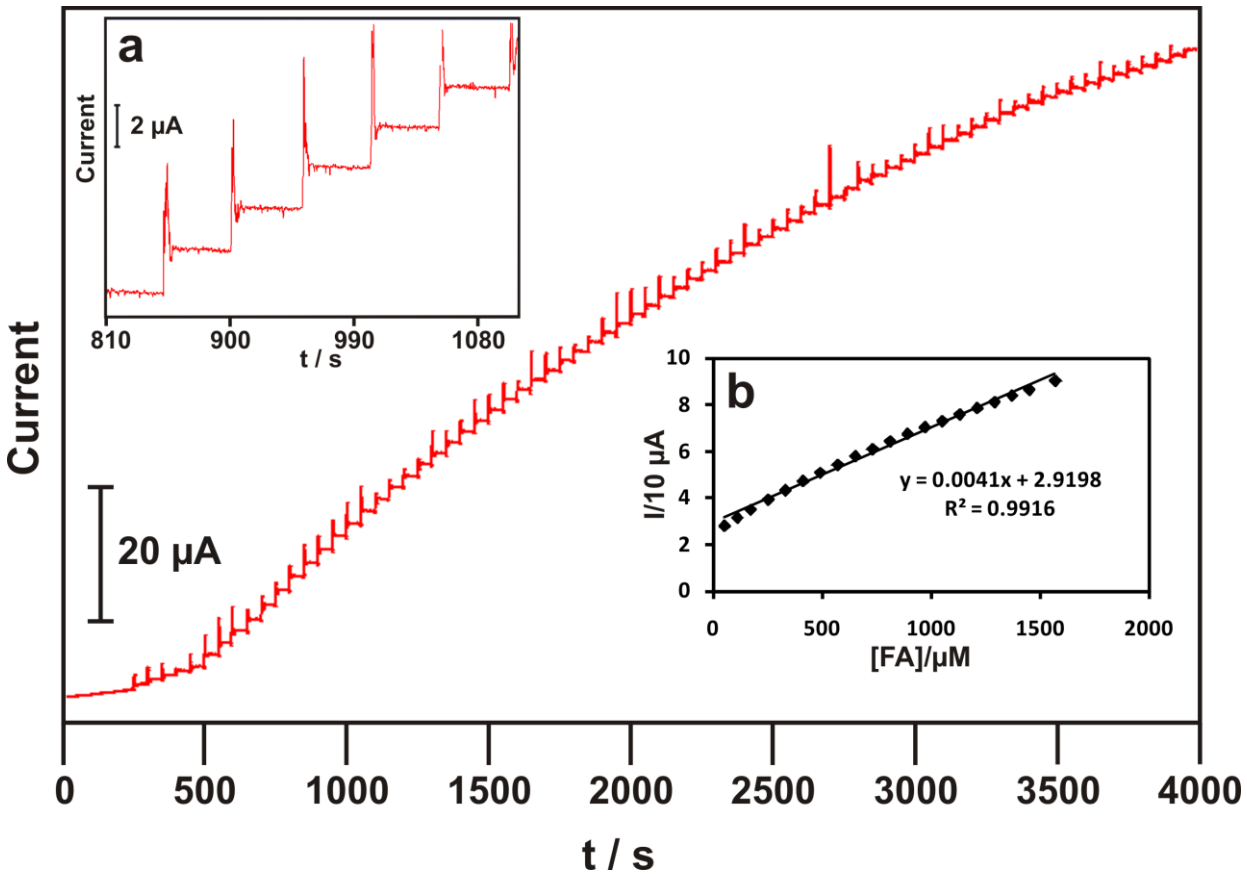

Figure 7. Amperometric i-t response at MWCNT-PVS modified rotating disc GCE (RDE) for the addition of 1.0×10^{-6} M to 2.74×10^{-3} M FA in N_2 saturated 0.1M PBS (pH 7). Applied potential: –0.7 V; Rotation rate: 900 RPM. Inset (a) is the enlarged view of the amperometric response in the linear range. Inset (b) shows the plot of linear dependence of current response to the concentration of FA in the linear range.

The inset (b) of fig. 7 shows the plot of dependence of current response to the concentration of FA in the linear range. The MWCNT-PVS/GCE shows a good linear range of 53μ M to 1.7 mM FA with a slope value of 0.041μA μM^{-1}. The correlation coefficient (R^2) was found to be 0.9916 and the sensitivity is 0.1737 μA μM^{-1} cm^{-2}. This shows the stability of the proposed electrode and the efficient amperometric response towards FA reduction. A comparison of linear range of FA determination at various electrodes from previous reports is given in Table 1.

Table 1. Comparison of linear range of determination of FA at various electrodes by various methods

Modified electrodes	Electrochemical methods	Linear range of detection	Ref.
[a]Gold electrode	Oxidative adsorptive stripping voltammetry	8.0×10^{-9} to 1.0×10^{-6} M	[6]
MWCNTs	Stripping voltammetry	3.00×10^{-7} to 8.00×10^{-5} M	[7]
Calixarene modified carbon paste electrode	Differential pulse adsorptive stripping voltammetry	8.79×10^{-12} to 1.93×10^{-9} M	[8]
(PMo_{12}) doped polypyrrole (PPy) film	DPV	1.0×10−8 to 1.0×10−7M	[12]
[b]Pencil graphite electrode	Differential pulse cathodic stripping voltammetry	0.007–0.156 μg mL^{-1}	[15]
MWCNT/Au	Chronoamperometry/ Chronocoulometry	2×10^{-8} M to 1×10^{-6} M.	[33]
Mercury electrode	AC adsorptive stripping voltammetry	1×10^{-8} to 1×10^{-11} M	[44]
[c]Carbon paste electrode	Differential pulse adsorptive stripping voltammetry	6×10^{-9} to 6×10^{-4} M	[45]
[d]SWCNT-ILPE	DPV	2.0×10^{-9} to 4.0×10^{-6} M	[46]
MWCNT- PVS/GCE	Amperometric i-t	5.3×10^{-5} M to 1.7×10^{-3} M	This work

[a]2-mercaptobenzothiazole self-assembled gold electrode

[b]Molecularly imprinted polymer-immobilized sol–gel-modified

[c]Carbon paste electrode modified with palmitic acid/stearic acid

[d] SWCNT-ionic liquid paste electrode

4. CONCLUSIONS

In the present study, we reported a simple procedure for GCE surface modification with MWCNT-PVS. The efficient electrocatalytic activity of the MWCNT-PVS film towards FA was revealed through CV and amperometric studies. We attempted the use of MWCNT-PVS for amperometric i-t curve studies for the determination of FA at –0.7 V and it was successfully demonstrated. The proposed film showed quick response and good linear range for FA detection. These results show the stability of the film and its promising and potential application in biosensor fabrication.

ACKNOWLEDGMENT
This project was supported by the National Science Council and the Ministry of Education of Taiwan (Republic of China).

References

1. C. M. Ulrich, *J. Nutr.,* 135 (2005) 2698.
2. L. E. Mitchell, N. S. Adzick, J. Melchionne, P. S. Pasquariello, L. S. Sutton and A. S. Whitehead, *The Lancet*, 364 (2004) 1885.
3. Y. Kim, *Cancer Epidemiol Biomarkers Prev*., 13 (2004) 511-519.
4. J. Y. Fang, S. Zhu, S. Xiao, S. Jiang, Y. Shi, X. Chen, X. Zhou and L. Qian, *J. Gastroen. Hepatol*., 11 (1996) 1079.
5. S. J. Duthie, S. Narayanan, G. M. Brand, L. Pirie and G. Grant, *J. Nutr.*, 132. 8 Suppl. (2002) 2444S.
6. Q. Wan and N. Yang, *J. Electroanal. Chem*., 527 (2002) 131.
7. X. Jiang, R. Li, J. Li and X. He, *Russ. J. Electrochem.*, 45 (2009) 772.
8. V. D. Vaze and A. K. Srivastava, *Electrochim. Acta*, 53 (2007) 1713.
9. S. Cakir, I. Atayman and O. Cakir, *Microchim. Acta*, 126 (1997) 237.
10. P. Kalimuthu and S. A. John, *Biosens. Bioelectron.*, 24 (2009) 3575.
11. Y. Umasankar, T. W. Ting and S. M. Chen, *J. Electrochem. Soc.*, 158 (2011) K117.
12. H. X. Guo, Y. Q. Li, L. F. Fan, X. Q. Wu and M. D. Guo, *Electrochim. Acta*, 51 (2006) 6230.
13. R. Ojani, J. Raoof and S. Zamani, *Electroanal.*, 21(2009) 2634.
14. A.A. Ensafi and H. K. Maleh, *J. Electroanal. Chem.*, 640 (2010) 75.
15. B. B. Prasad, R. Madhuri, M. P. Tiwari and P. S. Sharma, *Sens. Actuators B*, 146 (2010) 321.
16. A. R. Taheri1, A. Mohadesi, D. Afzali, H. K. Maleh, H. M. Moghaddam, H. Zamani, Z. R. Zad, *Int. J. Electrochem. Sci.*, 6 (2011) 171.
17. H. Yaghoubian, V. S. Nejad, S. Roodsaz, *Int. J. Electrochem. Sci.,* 5 (2010) 1411.
18. M. M. Ardakani1, R. Arazi1, H. Naeimi, *Int. J. Electrochem. Sci.,* 5 (2010) 1773.
19. H. Qi and C. Zhang, *Electroanal.*, 17 (2005) 832.
20. Z. Wang, S. Li and Q. Lv, *Sens. Actuators B*, 127 (2007) 420.
21. Y. Umasankar, A. P. Periasamy, S. M. Chen, *Anal. Biochem.*, 411 (2011) 71.
22. S.F. Wang and Q. Xu, *Anal. Lett.*, 38 (2005) 657.
23. L. Agui, P.Y. Sedeno and J. M. Pingarron, *Anal. Chim. Acta*, 622 (2008) 11.
24. U. Yogeswaran, S. M. Chen, *Electrochim. Acta*, 52 (2007) 5985.
25. U. Yogeswaran, S. M. Chen, *Sens. Actuators, B*, 130 (2008) 739.
26. J. F. Rusling, A. E. F. Nassar, *Langmuir*, 10 (1994) 2800.
27. A.E. F. Nassar, W. S. Willis and J. F. Rusling, *Anal. Chem.*, 67 (1995) 2386.
28. A.E. F. Nassar, J. M. Bobbitt, J. D. Stuart, J. F. Rusling, *J. Am. Chem. Soc.*, 117 (1995) 10986.

29. Q. Huang, Z. Lu and J. F. Rusling, *Langmuir,* 12 (1996) 5472.
30. N. Hu and J. F. Rusling, *Langmuir,* 13 (1997) 4119.
31. W. Cheng, G. Jin and Y. Zhang, *Sens. Actuators, B,* 114 (2006) 40.
32. Y. Zhang, Y. Cai and S. Su, *Anal. Biochem.,* 350 (2006) 285.
33. S. Wei, F. Zhao, Z. Xu and B. Zeng, *Microchim. Acta,* 152 (2006) 285.
34. D. R. S. Jeykumari, S. Ramaprabhu and S. S. Narayanan, *Carbon*, 45 (2007)1340.
35. H. Su, R. Yuan, Y. Chai, Y. Zhuo, C. Hong, Z. Liu and X. Yang, *Electrochim. Acta,* 54 (2009) 4149.
36. C. Wang, C. Li, L. Ting, X. Xu and C. Wang, *Microchim. Acta*, 152 (2006) 233.
37. R. C. Gurira, C. Montgomerya and R. Winston, *J. Electroanal. Chem.,* 333 (1992) 217.
38. A.C. L. Gall, C. M. G. Van den Berg, *Anal. Proc.*, 29 (1992) 201.
39. S. Cakir, E. Bicer, O. Cakır, *J. Inorg. Biochem.*, 77 (1999) 249.
40. E. Katz, I. Willner and *Electroanal.*, 15 (2003) 913.
41. H. O. Finklea, D. A. Snider and J. Fedyk, *Langmuir,* 9 (1993) 3660.
42. S. Chakraborty, C. R. Raj, *J. Electroanal. Chem.*, 609 (2007) 155.
43. A.J. Bard and L. R. *Faulkner, Electrochemical Methods Fundamentals and Applications*, 2nd ed., John Wiley & Sons, Inc, (2001) 331.
44. J. Han, H. Chen, H. Gao, *Anal. Chim. Acta*, 252 (1991) 47.
45. N. A. E. Maali, *Bioelectrochem. Bioenerg.*, 27 (1992) 465.
46. F. Xiao, C. Ruan, L. Liu, R. Yan, F. Zhao and B. Zeng, *Sens. Actuators B*, 134 (2008) 895.